RSC Advances

This is an *Accepted Manuscript*, which has been through the Royal Society of Chemistry peer review process and has been accepted for publication.

Accepted Manuscripts are published online shortly after acceptance, before technical editing, formatting and proof reading. Using this free service, authors can make their results available to the community, in citable form, before we publish the edited article. This *Accepted Manuscript* will be replaced by the edited, formatted and paginated article as soon as this is available.

You can find more information about *Accepted Manuscripts* in the Information for Authors.

Please note that technical editing may introduce minor changes to the text and/or graphics, which may alter content. The journal's standard Terms & Conditions and the Ethical guidelines still apply. In no event shall the Royal Society of Chemistry be held responsible for any errors or omissions in this *Accepted Manuscript* or any consequences arising from the use of any information it contains.

ROYAL SOCIETY OF CHEMISTRY

www.rsc.org/advances

RSC Advances

Cite this: DOI: 10.1039/c0xx00000x

www.rsc.org/xxxxxx

PAPER

Trap induced tunable unusual dielectric properties in transition metal doped reduced graphene oxide

Abu Jahid Akhtar, Abhisek Gupta and Shyamal K. Saha*

Received (in XXX, XXX) Xth XXXXXXXXX 20XX, Accepted Xth XXXXXXXXX 20XX
DOI: 10.1039/b000000x

Graphene being an excellent electronic material has poor dielectric property. In addition to unusual dielectric response (permittivity increases with frequency) due to trap induced capacitance, here we have tuned the trap states to achieve a giant value of permittivity (Ɛ~ 2214) and remarkably high magneto-dielectric effect (23%) in nickel doped reduced graphene oxide (RGO). The current-voltage characteristics in the space charge limited conduction give quantitative information about these traps states. We estimate an average trap density of 1.92×10^{22} m^{-3} at room temperature. We believe that this transition metal doped RGO with tunable dielectric has potential applications in electrical storage devices.

1 Introduction

Graphene, one-atom-thick two-dimensional layer of sp^2-bonded carbon, has attracted tremendous research interest in recent years owing to its remarkably high electrical and thermal conductivities, superior mechanical strength and very large specific surface area[1-5]. All these unique and extraordinary properties make graphene as a novel material for large variety of applications in spintronics[6-8], optoelectronics[9,10], sensors[11,12], batteries[13,14], supercapacitors[15-17] and hydrogen storage[18]. Several strategies [8,19-23] have already been developed to enhance the magnetic and optical properties however, no effect has yet to be explored to tune its dielectric properties in graphene for potential application in storage devices.

One of the finest ways to improve the magnetic property in graphene is the doping of transition metal (TM) atom[24,25]. The advantage of introduction of this TM atom is to create multifunctional property in graphene. This TM atom not only enhances the magnetic property but also creates remarkable dielectric properties[26] due to trap induced capacitance which is a unique feature in graphene. Theses trap states contribute to capacitance only if they are filled and as a result, the dielectric response can be tuned by controlling the characteristic feature of the traps produced due to the incorporation of TM atoms at the carbon vacancy.

The motivation of the present work is to enhance its dielectric response to a giant value (Ɛ~2214) with an additional aspect of remarkable magneto-dielectric effect (23% change in magneto-capacitance) just tuning the trap characteristics by proper choice of TM atom, for which we have used nickel atom in the present study. Analysis of temperature dependent current density (J)-voltage (V) study is also presented to elucidate the nature and density of trap states giving rise to this type of unusual dielectric response in which permittivity increases with frequency.

2 Experimental

2.1 Synthesis

In order to synthesize nickel doped reduced graphene oxide (Ni-RGO), in the first step we prepare graphene oxide from the natural graphite by modified hummers' method[27]. This freshly prepared 10ml of GO is dispersed in 100ml of N,N-dimethyl formamide (DMF) in an ultrasonic bath for 1h to get a homogeneous brown yellow coloured solution. Then 500mg of anhydrous nickel chloride dispersed in distilled water is added to this brown yellow coloured solution and stirred for 30min followed by ultrasonic vibration for 1h. In the last step, 15ml of hydrazine hydrate is added to the mixture at 60^0C and sonicate for 1h. The mixture is then filtered several times with distilled water and alcohol till the ethanol solution becomes colourless to get rid of all unwanted reactants. The final product is dried under vacuum at 150^0C for 24h to get the ultimate product named as Ni-RGO_1h. For the preparation of Ni-RGO_4h and Ni-RGO_6h all the procedures discussed above are same expect the last step. In the case for Ni-RGO_4h, after adding the hydrazine hydrate the mixture is sonicated for 4h and for Ni-RGO_6h the sonication time is 6h.

We further synthesize reduced graphene oxide (RGO_stir) by reduction of GO under stirring condition. For the preparation of RGO_stir, 10ml of GO is first dispersed in 100ml of DMF and stir for 2h to get a homogeneous mixture. 15ml of hydrazine hydrate is then added to it and stir for 6h at 60^0C. Finally the mixture is then filtered and dried at 150^0C to get the final product.

2.2 Characterization

For dielectric and magneto-dielectric measurements the as-synthesized powdered sample is pressed in the form of a pellet with 0.328 cm^2 area and 0.062 cm thickness. Using silver paste

RSC Advances Accepted Manuscript

on both sides of the pellet as electrodes the dielectric and magnetodielectric measurements are done by Agilent E4980A Precision LCR Meter and an electromagnet with field range up to 2T. The current-voltage (I-V) characteristics are measured by Keithley 2601 I-V source meter. Raman Measurements are carried out using LabSpec Raman spectroscope (Model JYT6400).The sample for Raman measurement is excited at 514 nm with an Ar-ion laser with a scanning duration of 50s. The X-ray photoelectron spectroscopy (XPS) measurements are performed using OMICRON-0571 system.

3 Results and discussion

Now we discuss the mechanism of formation for Ni-RGO sample. Fig. 1a shows the typical atomic configuration of Ni doped reduced graphene oxide.

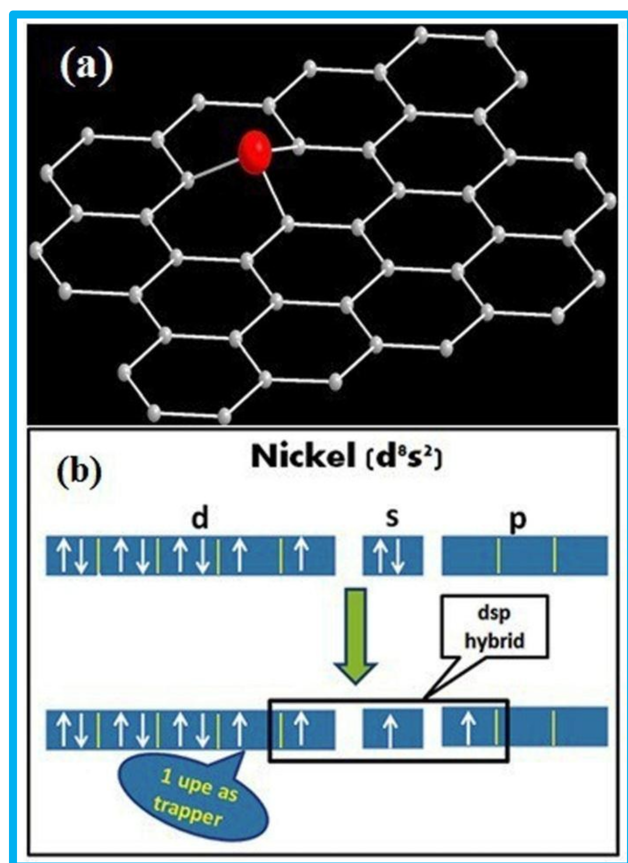

Fig. 1 (a) Typical atomic configuration of nickel atom embedded on the carbon vacancy site of graphene. (b) Schematic flow diagram of how trap is produced in graphene when nickel atom is embedded at the vacancy site.

During the sonication of GO solution, GO sheets are exfoliated and due to tremendous local heat which is generated during ultrasonic vibration removes some carbon atoms from the graphene lattice resulting the formation of some defect states. Now while adding nickel chloride into GO solution, some of the Ni^{2+} ions are incorporated at the defect sites of carbon vacancies. In the final stage after prolonged sonication using hydrazine hydrate, GO sheets are reduced with the reconstruction of carbon network structure with some vacancies occupied by nickel atoms. The electronic configuration of nickel atom is d^8s^2. When Ni atoms are placed in a single vacancy of defective graphene i.e., M/SV, one electron from s^2 configuration is promoted to next p level to achieve "spd" hybridization which takes part in the in-plane bonding with the three neighbouring carbon atoms[28].

This type of hybridization for M/SV leaves 7d electrons (3 paired and 1 unpaired). The unpaired electron occupying d_z^2 orbital is unable to take part in d-p mixing with the p_z orbital of neighbouring carbon atom. This unpaired electron of Ni atom together with electron present in the p_z orbital of neighbouring carbon atom act as trapping sites. Therefore, in case of nickel doped graphene, each nickel centre produces two trap states associated with one unpaired electron in the d_{z2} orbital of Ni atom and one unpaired electron in the p_z orbital of one carbon atom as shown in Fig. 1b.

Figs. 2a–2d show the XPS spectra which have been carried out to recognize the Ni doped graphene structure. Fig. 2a shows the peaks corresponding to binding energies (B.E.) at about 285 and 532eV which are assigned to C1s and O1s orbitals, respectively. The peaks in the marked portions in Fig. 2a represent the B.E. of Ni2s, 2p and 3p orbitals. Fig. 2b-d show the enlarged views of Ni2p, 3p and 2s peaks. The peaks in Fig. 2b at ~ 858.6, 875.9eV correspond to the B.E. of $Ni2p_{3/2}$ and $Ni2p_{1/2}$. In Fig. 2c, the peak ~71.5eV is assigned to Ni3p and in Fig 2(d), the peak ~ 1014.2eV is attributed to Ni2s. It is seen from the enlarged view of Ni2p, 3p and 2s peaks in Figs 2b-2d, all the B.E. peaks are shifted almost 6eV with respect to Ni. This is in conformation with the theoretical prediction[28] of shifting in B.E. due to doping of Ni atom at vacant sites of defective graphene.

Raman spectroscopy has been carried out in our as-synthesized sample as it plays an important role in providing the valuable information about structural defects of graphitic materials. The D and G bands for the Ni-RGO sample appear at 1348 and 1604cm^{-1} respectively. This D band is defect-induced Raman features and is absent in highly crystalline graphite. The integrated intensity ratio I_D/I_G for the D band and G band is widely used for characterizing the defect quantity in graphene based material.[29] This defect induced character is clearly observed in Fig. 2e. As evident from the figure for Ni-RGO_6h sample the I_D/I_G ratio is found to be 1.22 whereas for Ni-RGO_1h the ratio is found to be 1.06. We also perform the Raman study for the RGO_stir sample in which the intensity ratio I_D/I_G is found to be 0.92 which simply suggests that RGO_stir sample is much less defective than the Ni-RGO samples and the reason behind this is that in synthesizing RGO_stir sample no ultrasonic vibration is used. This observation clearly indicates that the defects are the manifestation of the sonication effect that is used during the synthesis of the samples and varying the sonication time we can introduce more and more defects in the sample.

RSC Advances Accepted Manuscript

 This journal is © The Royal Society of Chemistry [year]

RSC Advances

Dynamic Article Links ►

Cite this: DOI: 10.1039/c0xx00000x

www.rsc.org/xxxxxx

PAPER

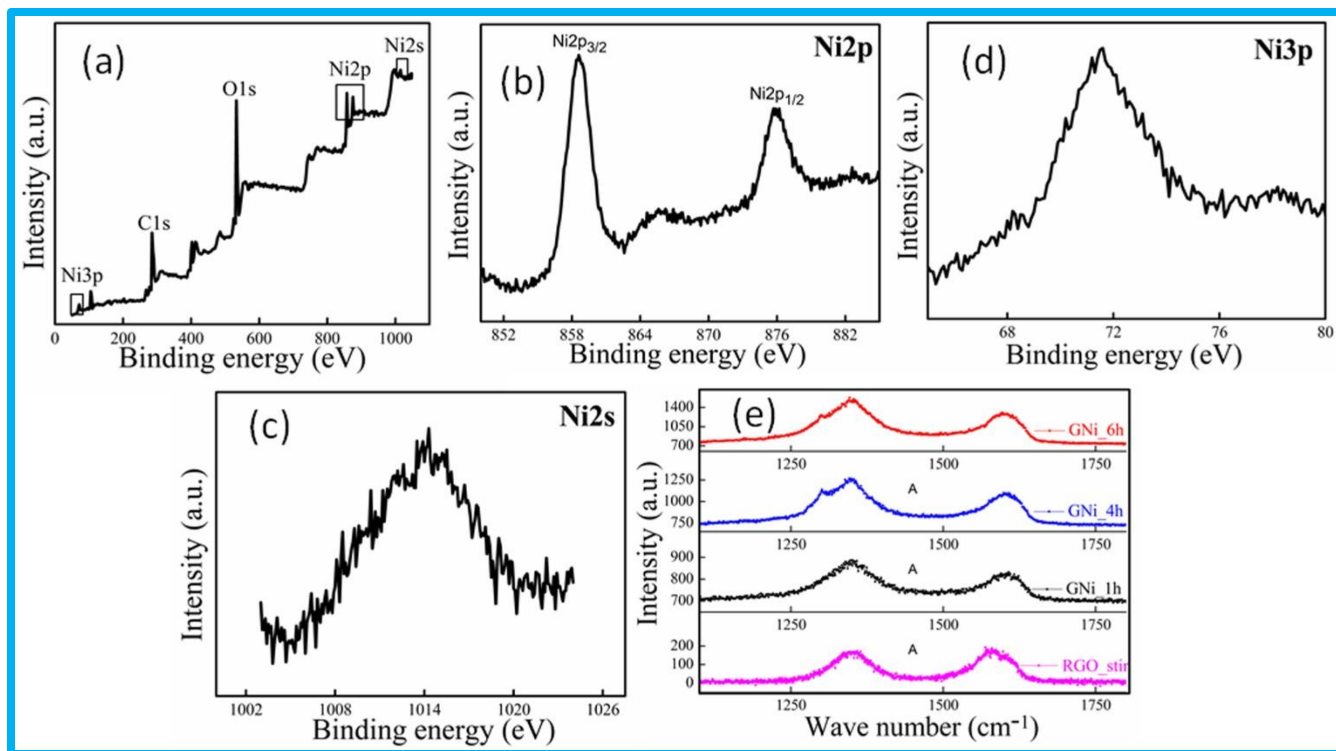

Fig. 2 (a) Full survey of XPS spectra for nickel doped reduced graphene oxide showing the peaks corresponding to binding energies of C1s, O1s, Ni3p, Ni2p and Ni2s orbitals (b) high resolution spectra for Ni2p orbitals (c) high resolution spectra for Ni3p and (d) high resolution survey for Ni2s. (e) Comparison of Raman spectra for Ni-RGO and RGO_stir samples with different sonication time. It appears that integrated intensity ratio I_D/I_G for the D band and G band increases with increase in sonication time.

Fig. 3a gives the temperature dependent current density (J)-Voltage (V) study for Ni doped reduced graphene oxide sample. One of the experimental methods for the detection of the trap states is the analysis of J-V study using space charge limited conduction (SCLC) mechanism. According to SCLC mechanism the expression for current density is given by[30]

$$J = \left(\frac{\mu N_v}{q^{l-1}}\right)\left(\frac{2l+1}{l+1}\right)^{1/l}\left[\left(\frac{\varepsilon\varepsilon_0}{N_t}\right)\left(\frac{l}{l+1}\right)\right]^{l}\left(\frac{V^{l+1}}{d^{2l+1}}\right) \quad \ldots\ldots\ (1)$$

Where q the electronic charge, $\varepsilon\varepsilon_0$ the dielectric constant, μ the free electron mobility, N_v the effective density of states, N_t the trap density of states and l is an exponent and must be greater than 1.

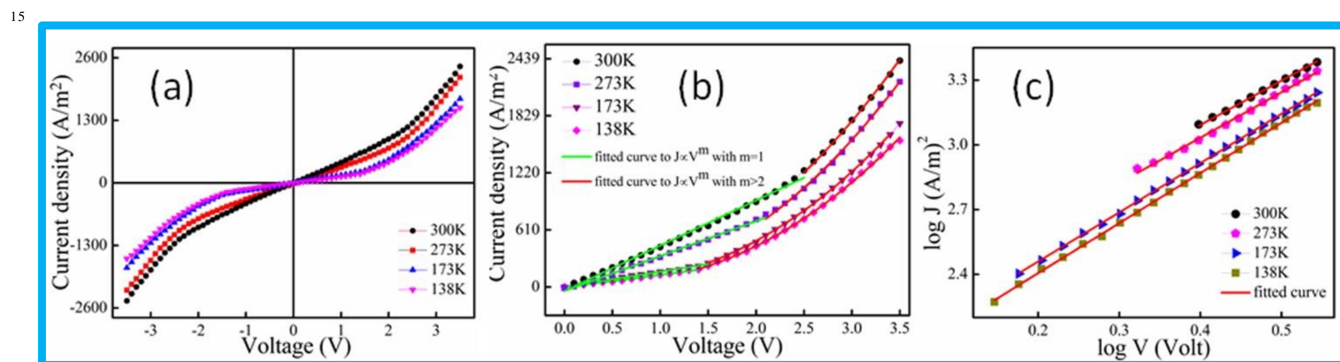

Fig. 3 (a) Current density (J) - Voltage (V) characteristics at different temperature for Ni-RGO_6h. (b) J-V curve at positive bias voltage fitted with $J \propto V^m$ showing ohmic and SCLC region. (c) Plot of logJ vs logV at different temperatures showing expand view of SCLC regime.

RSC Advances Accepted Manuscript

Fig. 3b shows the plot of J vs V at different temperatures and we explain our data using SCLC model to quantify the trap states. The solid green and red lines are a fit to $J \propto V^m$. At low bias voltage the conduction is ohmic with m=1(green solid line), whereas at higher bias voltage m deviates from 1 implying space charge limited conduction with exponential distribution of traps (red solid line). In order to get a rough estimate of trap density we have plotted logJ vs logV at higher bias voltage as shown in Fig. 3c and fitted the curves using equation (1). In this case, the conduction is mediated via exponentially distributed trap states. From this curve the average trap density at room temperature is found to be 1.92×10^{22} m^{-3}.

Fig. 4a gives the variation of dielectric permittivity as a function of frequency for the Ni-RGO samples sonicated at different time intervals. The interesting feature of this study is the increase in permittivity with frequency. At lower frequency region the increase is abrupt and continues to increase to high frequency region. Another interesting point to note that the dielectric function changes significantly with sonication time. For higher sonication time (higher dopant concentration) permittivity continues to increase beyond 2MHz while for lower sonication time (lower dopant concentration) it starts to decrease after 100kHz like other normal dielectrics.

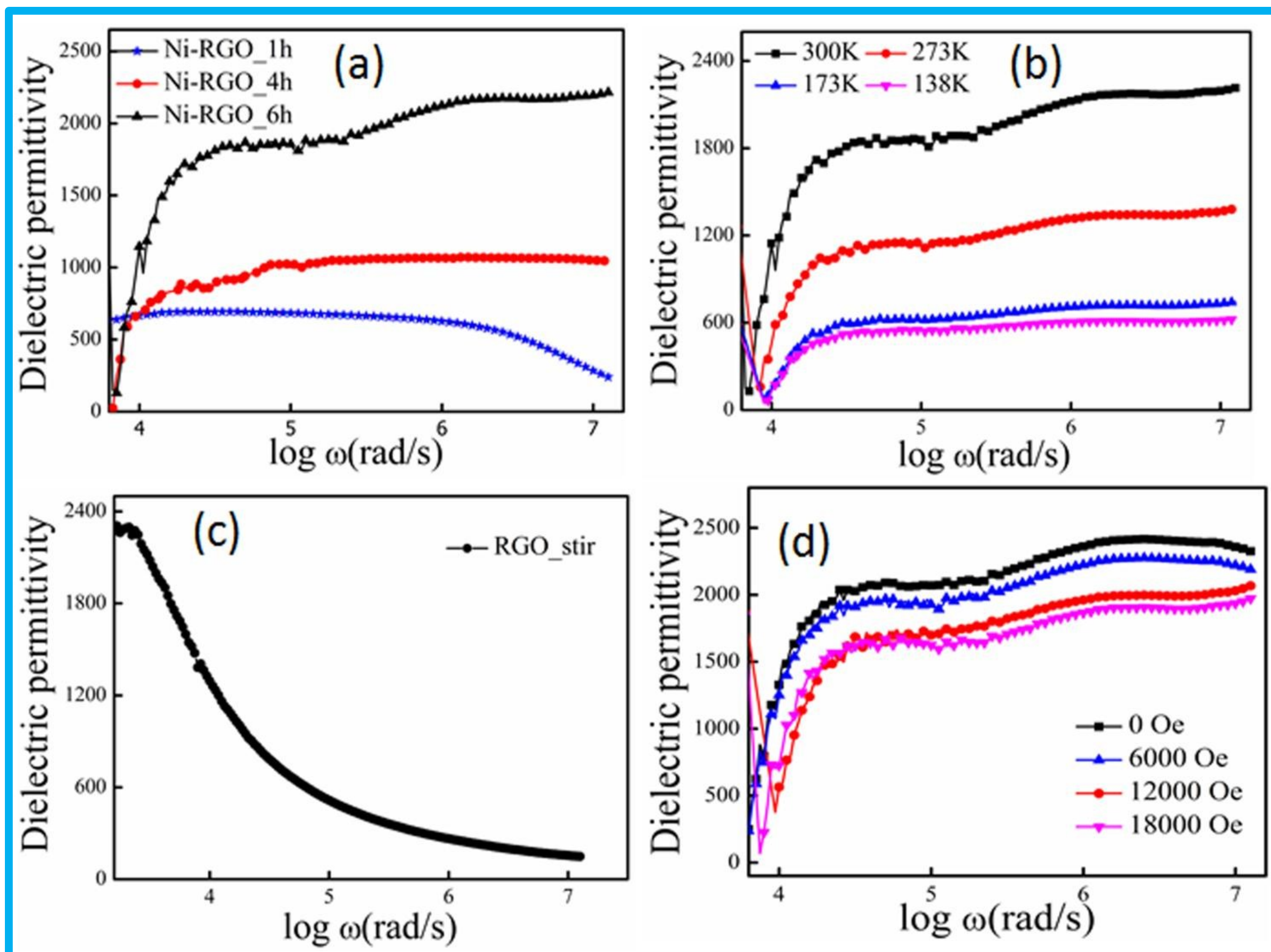

Fig. 4 (a) Variation of dielectric permittivity as a function of frequency for Ni-RGO samples. (b) Plot of permittivity with frequency for Ni-RGO_6h at different temperatures. (c) Variation of dielectric permittivity with frequency for RGO_stir sample at room temperature. (d) Comparision of dielectric permittivity with frequency for Ni-RGO_6h sample at different magnetic fields.

In order to explain this unusual dielectric response in our system, we have invoked the concept of trap centre at the dopant site as mentioned earlier. During the motion from one electrode to the other under bias voltage the electrons are trapped in the trap states and contribute to capacitance.

It is seen that each trap level represents a RC circuit with a characteristic trap frequency [31]

$$\omega_t \sim \frac{1}{R_{trap} * C_{trap}} \quad \text{....................................} \quad (2)$$

where R_{trap} represents the trap resistance and C_{trap} is the trap capacitance. This trap induced capacitance is very much different

RSC Advances Accepted Manuscript

This journal is © The Royal Society of Chemistry [year]

from ordinary dielectric capacitance where capacitance value decreases with frequency. In this case, the trap capacitance arises only when it is filled otherwise the empty traps do not contribute any capacitance. As is evident from literature that this characteristic trap frequency ω_t increases exponentially with trap energy (E_t) given by[31]

$$\omega_t \sim \omega_0 \exp\left[-\frac{E_c - E_t}{kT}\right] \text{ with } |E_t|>|E_c| \quad \ldots\ldots\ldots\ldots\ldots (3)$$

We have explained this unusual dielectric response considering the exponential distribution of traps as reported in the literature,[32]

$$n_t(E) \sim \frac{N_t}{kT_0}\exp\left[-\frac{E_t - E_c}{kT}\right] \text{ with } |E_t| > |E_c| \ldots\ldots\ldots\ldots (4)$$

where N_t is the total volume density of traps, E_c is the conduction band edge and T_0 is a parameter that gives the depth of the distribution and k is the Boltzmann constant. From this equation it is seen that the density of shallow traps is the maximum and it decrease exponentially with trap energy.

For any fixed temperature, the mobility of conduction electrons remains constant and when dc bias is applied very few electrons are trapped only in the deep trap levels and contribute to small capacitance. However, under application of ac field the probability of electrons being trapped in the comparatively less deeper traps is increased due to "to and fro" motion of the electrons. With increase in frequency more and more electrons are trapped in the shallow trap levels and capacitance increases with frequency as shown in Fig. 4a. When all the traps are filled by the electrons the capacitance become saturated and finally starts to decrease with frequency as in ordinary dielectric. Fig. 4b shows the temperature dependent permittivity-frequency study for the Ni-RGO_6h sample. It is evident from the figure that the permittivity value decreases with decrease in temperature. This is because of two reasons. Firstly, at low temperature most of the traps are filled and highly localized. Secondly, mobility of conduction electrons is relatively high. As a result, at relatively low temperature, the probability of conduction electrons getting trapped decreases and as a consequence capacitance value decreases with decrease in temperature.

In order to check this unusual behaviour as a result of trap states that produced due to defect states created in graphene, we also study the permittivity value with frequency for RGO_stir sample at room temperature. As evident from Raman study that the major difference of RGO_stir sample from other samples mentioned earlier is the presence of defect states. Less defect means less amount of trap states. It means that the contribution of trap states towards capacitance is negligible in case of RGO_stir sample. As the permittivity value starts to decrease from a very low frequency and continues to decrease upto highest frequency as shown in Fig. 4c and giving a very low value of dielectric permittivity ($\varepsilon \sim 149$) at 2MHz.

Another important issue in the present Ni-RGO sample is the appearance of very large magneto-dielectric effect (23%) as shown in Fig. 4d. The origin of this large decrease in dielectric permittivity under the application of magnetic field lies with the fact that in Ni-RGO sample each Ni centre produces two trap states which contain two unpaired electrons carrying each a spin ½ moment. Under the application of magnetic field both the spins are aligned in the direction of magnetic field and the probability of conduction electrons which are also partially polarized in the same direction being trapped in the trap centres decreases significantly with magnetic field. Therefore, the present study indicates that by proper choice of transition metal atom the trap states in reduced graphene oxide can be tuned to create giant dielectric permittivity and magneto-dielectric effects which have potential applications in graphene based storage devices.

Conclusions

In conclusion, transition metal doped reduced graphene oxide emerges as a new class of materials which show giant permittivity as well as fairly large magneto-dielectric effect. The high value of dielectric permittivity and remarkable magneto-dielectric effect are explained on the basis of trap states that are created due to doping of Ni atoms in the graphene. The major finding of this material is the tuning of dielectric responses with trap states that are created during sonication time. We strongly believe that these materials with tunable dielectric property will have enormous applications in graphene based storage devices.

Acknowledgements

AJA and AG acknowledge DST, New Delhi and CSIR for awarding the fellowships during the work. SKS acknowledges DST, New Delhi, Govt. of India for financial support, Project No. SR/NM/NS-1089/2011 and DST unit on Nanoscience for providing XPS facilities.

Notes and references

Department of Materials Science
Indian Association for the Cultivation of Science
Jadavpur, Kolkata, 700032, India
; E-mail address of corresponding author: cnssks@iacs.res.in

1 A. K. Geim, *Science*, 2009, **324**, 1530.
2 C. Lee, X. Wei, J. W. Kysar and J. Hone, *Science,* 2008, **321**, 385.
3 A. K. Geim and K. S. Novoselov, *Nat. Mater.*, 2007, **6**, 183.
4 A. A. Balandin, S. Ghosh, W. Bao, I. Calizo, D. Teweldebrhan, F. Miao and C. N. Lau, *Nano Lett.*, 2008, **8**, 902.
5 A. Das, S. Pisana, B. Chakraborty, S. Piscanec, S. K. Saha, U. V. Waghmare, K. S. Novoselov, H. R. Krishnamurthy, A. K. Geim, A. C. Ferrari and A. K. Sood, *Nature Nanotech.,* 2008, **3,** 210.
6 S. Mandal and S. K. Saha, *Nanoscale*, 2012, **4**, 986.
7 D. Soriano, F. Muñoz-Rojas, J. Fernández-Rossier and J. J. Palacios, *Phys. Rev. B*, 2010, 81, 165409.
8 S. K. Saha , M. Baskey and D. Majumdar, *Adv. Mater.*, 2010, 22, 5531.
9 A. Gupta and S. K. Saha, *Nanoscale*, 2012, **4**, 6562.
10 F. Bonaccorso, Z. Sun, T. Hasan and A. C. Ferrari, *Nature Photon.*, 2010, **4,** 611.
11 B. Zhang and T. Cui, *Appl. Phys. Lett.*, 2011, **98**, 073116 (2011).
12 Z. Cheng, Q. Li, Z. Li, Q. Zhou and Y. Fang, *Nano Lett.*, 2010, **10**, 1864.
13 E. Yoo, J. Kim, E. Hosono, H. S. Zhou, T. Kudo and I. Honma, *Nano Lett.*, 2008, **8**, 2277.
14 G. Wang, X. Shen, J. Yao and J. Park, *Carbon*, 2009, **47**, 2049.

RSC Advances Accepted Manuscript

15 N. G. Sahoo, Y. Pan, L. Li and S. H. Chan, *Adv. Mater.*, 2012, **24**, 4203.
16 G. Guo, L. Huang, Q. Chang, L. Ji, Y. Liu, Y. Xie, W. Shi and N. Jia, *Appl. Phys. Lett.*, 2011, **99**, 083111.
17 A. Gupta, A. J. Akhtar and S. K. Saha, *Mater. Chem. Phys.*, 2013, **140**, 616.
18 C. Ataca, E. Aktürk, S. Ciraci and H. Ustunel, *Appl. Phys. Lett.*, 2008, **93**, 043123.
19 J. Zhou, M. M. Wu, X. Zhou and Q. Sun, *Appl. Phys. Lett.*, 2009, **95**, 103108.
20 S. Mandal, M. Baskey, and S. K. Saha, *Carbon*, 2013, **61**, 254.
21 Y. Xu, Z. Liu, X. Zhang, Y. Wang, J. Tian, Y. Huang, Y. Ma, Xi. Zhang, and Y. Chen, *Adv. Mater.*, 2009, **21**, 1275.
22 (a) A. Gupta, B. K. Shaw and S. K. Saha, *J. Phys. Chem. C*, 2014, **118**, 6972 ; (b) A. Gupta, B. K. Shaw and S. K. Saha, *RSC Adv.*, 2014, **4**, 50542.
23 S. Mandal and S. K. Saha, *Appl. Phys. Lett.*, 2014, **105**, 022402.
24 C. Cao, M. Wu, J. Jiang, and H. P. Cheng, *Phys. Rev. B*, 2010, **81**, 205424.
25 H. Sevinçli, M. Topsakal, E. Durgun, and S. Ciraci, *Phys. Rev. B*, 2008, **77**, 195434.
26 A. J. Akhtar, A. Gupta, B. K. Shaw and S. K. Saha, *Appl. Phys. Lett.*, 2013, **103**, 242902.
27 W. S. Hummers and R. E. Offeman, *J. Am. Chem. Soc.*, 1958, **80**, 1339.
28 A. V. Krasheninnikov, P. O. Lehtinen, A. S. Foster, P. Pyykkö, and R. M. Nieminen, *Phys. Rev. Lett.*, 2009, **102**, 126807.
29 M. A. Pimenta, G. Dresselhaus, M. S. Dresselhaus, L. G. Cancado, A. Jorio and R. Saito, *Phys. Chem. Chem.Phys.*, 2007, **9**, 1276.
30 D. Joung, A. Chunder, L. Zhai, and S. I. Khondaker1, *Appl. Phys. Lett.*, 2010, **97**, 093105.
31 J. Bisquert, *Phys. Rev. B*, 2008, **77**, 235203.
32 J. Bisquert, F. Fabregat-Santiago, I. Mora-Seró, G. GarciaBelmonte, E. M. Barea and E. Palomares, *Inorg. Chim. Acta*, 2008, **361**, 684.

Table of Content

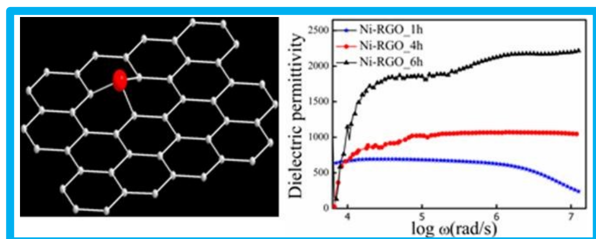

Giant value of permittivity (Ɛ~2214) and remarkably high magneto-dielectric effect (23%) are observed in nickel doped reduced graphene oxide (RGO).

RSC Advances Accepted Manuscript